International Journal of Nanomedicine

Dovepress
open access to scientific and medical research

Open Access Full Text Article

ORIGINAL RESEARCH

Fractionated photothermal therapy in a murine tumor model: comparison with single dose

This article was published in the following Dove Press journal:
International Journal of Nanomedicine

Marina Simón[1]
Kamilla Norregaard[1]
Jesper Tranekjær Jørgensen[1]
Lene Broeng Oddershede[2]
Andreas Kjaer[1]

[1]Department of Clinical Physiology, Nuclear Medicine & PET and Cluster for Molecular Imaging, Department of Biomedical Sciences, Rigshospitalet and University of Copenhagen, Copenhagen, Denmark; [2]Niels Bohr Institute, University of Copenhagen, Copenhagen, Denmark

Purpose: Photothermal therapy (PTT) exploits the light-absorbing properties of nanomaterials such as silica-gold nanoshells (NS) to inflict tumor death through local hyperthermia. However, in in vivo studies of PTT, the heat distribution is often found to be heterogeneous throughout the tumor volume, which leaves parts of the tumor untreated and impairs the overall treatment outcome. As this challenges PTT as a one-dose therapy, this study here investigates if giving the treatment repeatedly, ie, fractionated PTT, increases the efficacy in mice bearing subcutaneous tumors.

Methods: The NS heating properties were first optimized in vitro and in vivo. Two fractionated PTT protocols, consisting of two and four laser treatments, respectively, were developed and applied in a murine subcutaneous colorectal tumor model. The efficacy of the two fractionated protocols was evaluated both by longitudinal monitoring of tumor growth and, at an early time point, by positron emission tomography (PET) imaging of ^{18}F-labeled glucose analog ^{18}F-FDG.

Results: Overall, there were no significant differences in tumor growth and survival between groups of mice receiving single-dose PTT and fractionated PTT in our study. Nonetheless, some animals did experience inhibited tumor growth or even complete tumor disappearance due to fractionated PTT, and these animals also showed a significant decrease in tumor uptake of ^{18}F-FDG after therapy.

Conclusion: This study only found an effect of giving PTT to tumors in fractions compared to a single-dose approach in a few animals. However, many factors can affect the outcome of PTT, and reliable tools for optimization of treatment protocol are needed. Despite the modest treatment effect, our results indicate that ^{18}F-FDG PET/CT imaging can be useful to guide the number of treatment sessions necessary.

Keywords: hyperthermia, cancer, nanoparticle, photothermal therapy, fractionated therapy, positron emission tomography

Introduction

For years there has been growing interest in utilizing nanomedicine in cancer diagnostics and therapy.[1,2] One emerging approach within cancer nanomedicine is photothermal therapy (PTT). PTT relies on light-absorbing nanoparticles which are able to transform light into heat when irradiated with a resonant external light source, thereby causing tumor death through local hyperthermia.[3,4] To achieve efficient delivery of light to a nanoparticle-laden tumor and minimize unspecific heating, near-infrared (NIR) laser light is commonly used as it has the lowest absorption and deepest penetration in tissue.[5] Delivery of nanoparticles to the tumor tissue is in general based on passive accumulation facilitated through the enhanced permeability and retention (EPR) effect, which is a consequence of the leaky character of tumor

Correspondence: Andreas Kjaer
Department of Clinical Physiology, Nuclear Medicine & PET and Cluster for Molecular Imaging, Department of Biomedical Sciences, Rigshospitalet and University of Copenhagen, Nørre Allé 14, 2200 København N, 12.3, Copenhagen, Denmark
Email akjaer@sund.ku.dk

submit your manuscript | www.dovepress.com
DovePress
http://doi.org/10.2147/IJN.S205409

vessels and poor lymphatic drainage.[6–8] Because the individual components of the therapy are unharmful (the nanoparticles are inert and biocompatible, and the applied NIR laser dose is non-phototoxic), the therapeutic effect is only achieved in the tumor where the two are combined, making PTT highly controlled and localized.

Despite its promising capability to selectively ablate malignant tissue, PTT is still a fairly new approach that in most cases only has been performed successfully on animals with very small tumors.[9–13] Eradicating larger and more clinically relevant tumors without recurrence has proven more difficult.[14,15] One major reason for this is that larger tumors generally contain hypoxic regions with reduced blood perfusion, and this, together with high interstitial pressure, prevents nanoparticle delivery. The uneven nanoparticle distribution and the limited laser penetration depth lead to inhomogeneous intratumoral heat distribution during PTT, which also decays from the dermal surface in the direction of the externally applied laser and makes it difficult to ablate all cancer cells simultaneously.[16] Circumventing these challenges is not an easy fix, and brings up the question if the standard treatment protocol for PTT provides sufficient therapeutic efficacy for clinical applications. This has motivated researchers into studying an alternative use of PTT for combination therapies, for example to enhance chemotherapeutic efficacy, to release anticancer agents, or to induce an immune response for immunotherapy.[9,17–20] There are also approaches where enhanced irradiation doses are enabled by combining indirect heating of the tumor with tissue surface cooling, thereby preventing unspecific heating and treatment-associated pain.[21] Another strategy that has been suggested is to give the treatment in low-dose fractions instead of a single-dose, thereby killing cancer cells that survived the first treatment in following treatments and avoiding surface overheating.[22–26]

In a recent study,[27] we used PTT to treat mice-bearing subcutaneous murine colon carcinoma tumors (CT26 tumors) using NIR resonant silica-gold nanoshells (NS), which are the most widely used nanoparticles for both preclinical studies and clinical trials of PTT.[28–32] We found that, in spite of reaching temperatures during treatment that were above the threshold for cellular ablation, it did not result in complete tumor removal in more than a few mice. Furthermore, we observed unspecific heating in laser irradiated control groups of up to 45°C, preventing us from increasing the laser dose even further to enhance the treatment response. Hence, in this study we investigated in the same model and setup if there is a benefit of giving fractionated treatments. We first examined the ability of the NS to heat under different laser intensities in an in vitro setup, and confirmed that they could in fact undergo repeated heating sessions, a requirement for fractionated therapy. Following this, we investigated if unspecific heating could be eliminated by the use of an index matching agent in NIR irradiated tumors in mice. Finally, we evaluated and compared the treatment effect of two different protocols for fractionated PTT in tumor-bearing mice, using either two or four repeated treatment sessions. In addition, as our previous study showed that ^{18}F-fluorodeoxyglucose (^{18}F-FDG) positron emission tomography/computed tomography (PET/CT) imaging could be used for early non-invasive monitoring of PTT outcome,[33] this was implemented for evaluation of the fractionated protocols.

Materials and methods

Nanoparticles

The 800 nm Resonant BioPure™ Gold NS, consisting of a silica core surrounded by a thin gold shell, were obtained from NanoComposix, USA. The NS were functionalized with 5 kDa poly(ethylene glycol).

For the in vitro experiments, lot number JLF0015 was used. The total diameter of the NS detected through transmission electron microscopy (TEM) was reported by the supplier as 150±9 nm, the diameter of the silica core was 119±5 nm, and the zeta potential was −34 mV.

Lot number JCP1545 was used for the animal experiments. The total diameter of the particles was reported as 157±9 nm, and the diameter of the silica core was 119 nm±5 nm, with a zeta potential of −42 mV.

In vitro experiments

To study the heating ability of NS under NIR light in vitro, a solution of 5×10^9 NS/mL in water was prepared in a 1 mm plastic cuvette. The cuvette was placed under the laser beam, and the sample irradiated for 10 minutes at three different laser powers (1.2, 1.5, and 1.8 W/cm^2). Thereafter the solution was left to cool off for another 10 minutes. To study if the NS could be reheated, a sample was prepared containing 5×10^9 NS/mL, and four cycles of irradiation of 10 minutes each followed by 10 minutes of cooling off were performed (laser intensity of 1.5 W/cm^2). Afterwards, the sample was collected and TEM performed by qualified personnel at the Core Facility for Integrated Microscopy, Panum Institute, University of Copenhagen. For both in vitro studies,

the temperature in the solution was monitored real-time using thermographic imaging, where images were taken every 30 seconds with a thermal camera (FLIR T-440 camera). The images were analyzed within the FLIR tools software. For the UV-vis spectra, 20 µL of the stock solution of nanoparticles were dissolved in 4 mL of water. Measurements were performed using a Cary 5,000 UV-Vis-NIR Spectrophotometer (Agilent Technologies).

Animal model

The animal experiments were approved by the Danish Animal Welfare Council, Ministry of Justice, and undertaken in compliance with the directive 2010/63/EU of the European Parliament on the protection of animals used for scientific purposes. The animals used were 5-week-old female BALB/c mice from Charles River Laboratories (Wilmington, MA, USA). CT26 cells (ATCC) were cultured in RPMI 1640+ GlutaMAX™ medium, supplemented with 10% fetal bovine serum and 1% penicillin-streptomycin (Thermo Fisher Scientific) at 37°C and in 5% CO_2. When the cells reached ~70% confluence they were trypsinized and harvested. 3×10^5 cells (in 100 µL) were injected into the left flank of each mouse with a 27G needle. Mice were kept under anesthesia throughout the procedure by breathing 3–5% sevoflurane (Abbott Scandinavia AB, Sweden) mixed with 35% O_2 in N_2. Water and chow were available ad libitum. Animals were observed daily, and the tumor size measured every second or third day with a caliper. The tumor volume was calculated as: volume=½ (lengthxwidth^2). When the tumors reached 1,000 mm^3 the animals were euthanized.

Photothermal therapy

Mice were injected with 190 µL of either NS ($5x10^{10}$ NS/mL) or saline through the tail vein 24 hours before the first laser treatment, as this is a standard time point used in the literature with NS.[12,28,33,34] They were kept anesthetized with sevoflurane as previously described during the injection. The following day, mice were placed on a platform below an 807-nm laser beam (beam diameter of ~1 cm) and on a heating pad to maintain their body temperature. The laser intensity used was 1.2 W/cm^2. During the 5-minute irradiation, the temperature on the tumor surface was recorded using real-time thermographic imaging every 30 seconds (FLIR T-440 camera). For protocols where more than one laser treatment was applied, this process was repeated. When glycerol was applied, it was swabbed on the tumor right before the laser was turned on and after the treatment it was removed with ethanol and water. The animals were provided pain relief with temgesic (0.3 mg/mL) every 6–8 hours for 24 hours, starting immediately before the treatment, to avoid unnecessary distress. It was also decided to allow 1 day of recovery in between treatments due to the weight loss caused by the analgesia.[35] Day 60 was considered the end of the study, and tumor free animals were euthanized on this day. FLIR images were analyzed within the software FLIR tools.

PET/CT

^{18}F-FDG was produced at the Department of Clinical Physiology, Nuclear Medicine, and PET, Rigshospitalet, Centre of Diagnostic Investigations, Copenhagen, Denmark. ^{18}F-FDG PET scans were performed on a MicroPET Focus 120 scanner (Concorde Microsystems Inc., Knoxville, TN, USA) and CT scans were performed on a nanoScan SPECT/CT scanner (Mediso Medical Imaging Systems, Budapest, Hungary).

Approximately 10 MBq of ^{18}F-FDG were injected into the tail vein 1 hour before the PET scan. Mice were kept anesthetized with sevoflurane throughout the duration of the experiment, and their temperature maintained using a heating pad. The parameters used for the CT scan were the following: 720 projections, 300 ms of exposure time, and 35 kVp of x-ray energy. The parameters for the PET scan were: 300 seconds of acquisition time, energy window of 350–650 keV, and a timing window of 6 nanoseconds. Raw PET data was post-processed into sinograms and reconstructed using the maximum a posteriori (MAP) algorithm. MicroPET and CT images were manually fused using the Inveon software (Siemens Medical Solutions). The activity in the tumor was quantified by defining a region of interest (ROI) on the fused PET/CT images.

Data analysis and statistics

Survival curves were created using the Kaplan-Meier method, and median survival and hazard ratios (HR) were compared using the log-rank test. Two-way ANOVA with Tukey's multiple comparisons test was employed to compare the mean ^{18}F-FDG uptake. The mean maximum temperatures (at the last time point, 5 minutes) were compared using an unpaired two-tailed *t*-test or one-way ANOVA. Correlations between ^{18}F-FDG uptake and survival were calculated using linear regression, and the 95% confidence bands of the best-fit line were represented. The data was plotted in GraphPad Prism7 and shown as mean±SEM (standard error of the mean). Growth curves are shown until n=3.

Results

Heating properties of NS

First, we examined in vitro the heating properties of NS at different laser intensities, in the low range of what is commonly used for PTT.[36,37] A solution of 5×10^9 NS/mL in water was prepared in a plastic cuvette. The sample was irradiated from the top for 10 minutes with a laser intensity of 1.8, 1.5, or 1.2 W/cm^2, after which it was allowed to cool off for 10 minutes. With thermographic imaging we observed that the maximum temperatures reached were well above the threshold for induction of irreversible cellular damage for all laser intensities included (maximum temperatures of ~69°C at 1.8 W/cm^2, ~62°C at 1.5 W/cm^2, and ~58°C at 1.2 W/cm^2, Figure 1A).

Following this, another sample was irradiated in four cycles to test if the NS were photostable at these laser intensities. Figure 1B shows that, using a laser intensity of 1.5 W/cm^2, the sample could be reheated over intervals of 10 minutes, reaching maximum temperatures of ~65°C during the first cycle, ~66°C during the second, ~66°C during the third, and ~66°C during the fourth cycle of irradiation. Finally, we confirmed the optical absorption properties of the NS in the NIR region by measuring their UV-vis spectrum in a spectrophotometer (Figure 1C).

Glycerol as an index matching agent to reduce unspecific heating

In our previous studies of PTT in tumor-bearing animals,[27,33] it was observed that the laser in itself could induce an unspecific temperature increase of ΔT ~10°C, which could likely be attributed to laser attenuation in the dermal layer. In the early literature of in vivo PTT, it was mentioned that glycerol, as an index matching agent, can be swabbed onto the tumor prior to irradiation to enhance transdermal laser penetration.[11,12] Hence, we investigated if this method could reduce unspecific heating for different tumor sizes. Tumor-bearing mice were divided into three groups according to their tumor volumes; 100, 300, and 500 mm^3 (±20 mm^3 and n=4 for each group). The mice were injected with 190 µL of saline through the tail vein and after 24 hours irradiated for 5 minutes with NIR light covering the whole tumor using a laser intensity of 1.5 W/cm^2. Figure 2 shows the maximum temperature reached with and without the use of glycerol on the tumor. Without applying glycerol before irradiation (Figure 2A), the large tumors (ie, 500 mm^3) reached a maximum temperature increase of ΔT ~20°C, and the smaller tumors (ie, 100 and 300 mm^3) reached ΔT ~10°C. When glycerol was applied (Figure 2B), the maximum temperatures reached by the 500 mm^3 tumors were reduced considerably (to ΔT ~10°C). In contrast, the smaller tumors (100 and 300 mm^3) still reached a temperature increase of ΔT ~10°C. This, however, occurred at a slower rate, which also effectively reduces the integrated intensity and overall accumulated damage.

Evaluation of two-dose fractionated treatment in tumor-bearing mice

After studying the ability of the NS to be reheated and optimizing laser penetration using glycerol, the first protocol for fractionated PTT that we investigated was a two-dose fractionated treatment. Two groups of tumor-bearing mice were established and underwent either one laser ablation (NS1; n=5 and mean tumor size at baseline =143.2 mm^3),

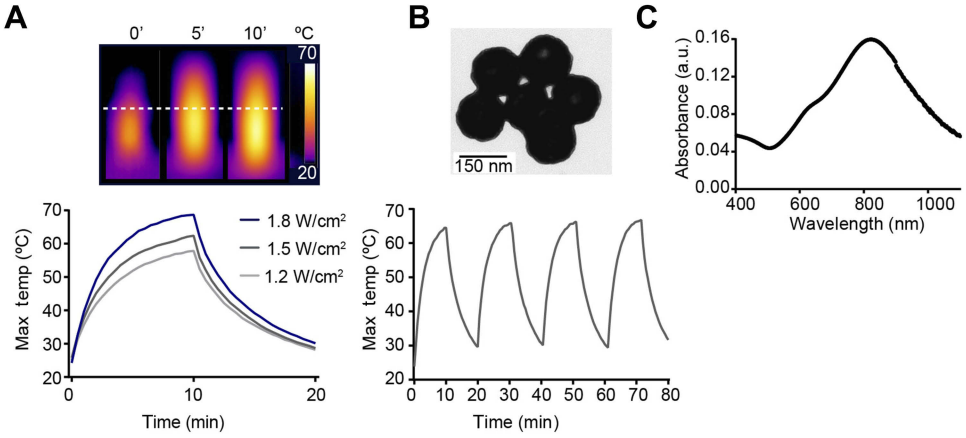

Figure 1 Heating of aqueous solution of NS under NIR light. (**A**) Thermographic imaging and temperature elevation as a function of time and laser intensity of a 5×10^9 NS/mL aqueous solution of NS. The dashed line represents the top of the sample. (**B**) Temperature elevation of a 5×10^9 NS/mL aqueous solution of NS irradiated in four cycles at a laser intensity of 1.5 W/cm^2. Inset shows a TEM image of intact NS after second cycle of heating. (**C**) Absorption spectrum of NS measured in water.

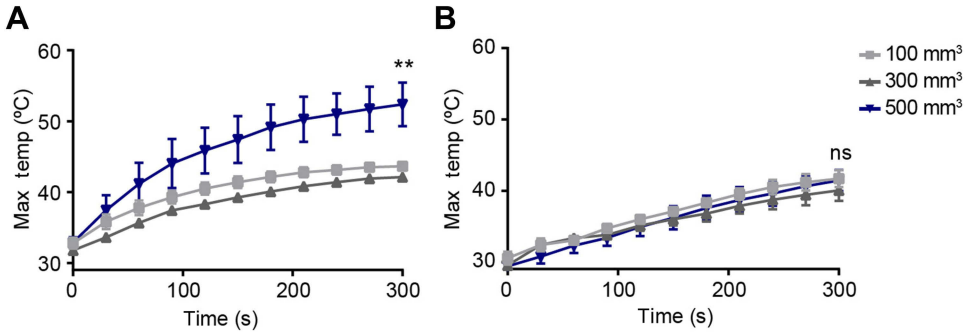

Figure 2 Reduction of unspecific heating using glycerol. (**A**) Temperature elevation on the tumor surface in the absence of glycerol as a function of time and tumor size. (**B**) Temperature elevation on the tumor surface in the presence of glycerol as a function of time and tumor size. Temperatures on the last time point (300 s) were compared between the 500 mm^3 and both smaller groups. ** Denotes a p value <0.01.
Abbreviation: ns, non-significant.

or two laser ablations with 1 day in between (NS2; n=6 and mean tumor size at baseline=136.1 mm^3). In addition, two control groups were also included, representing tumor-bearing mice injected with saline and irradiated once (Saline1; n=8 and mean tumor size at baseline=126.7 mm^3) or twice with 1 day in between (Saline2; n=6 and mean tumor size at baseline=120.4 mm^3), and finally a sham group that received NS but no photothermal ablation (Sham, n=6 and mean tumor size at baseline=107.4 mm^3). The experimental timeline is shown in Figure 3A. All the animals were injected with NS or saline 24 hours before the first treatment, and irradiated for 5 minutes with a laser intensity of 1.2 W/cm^2.

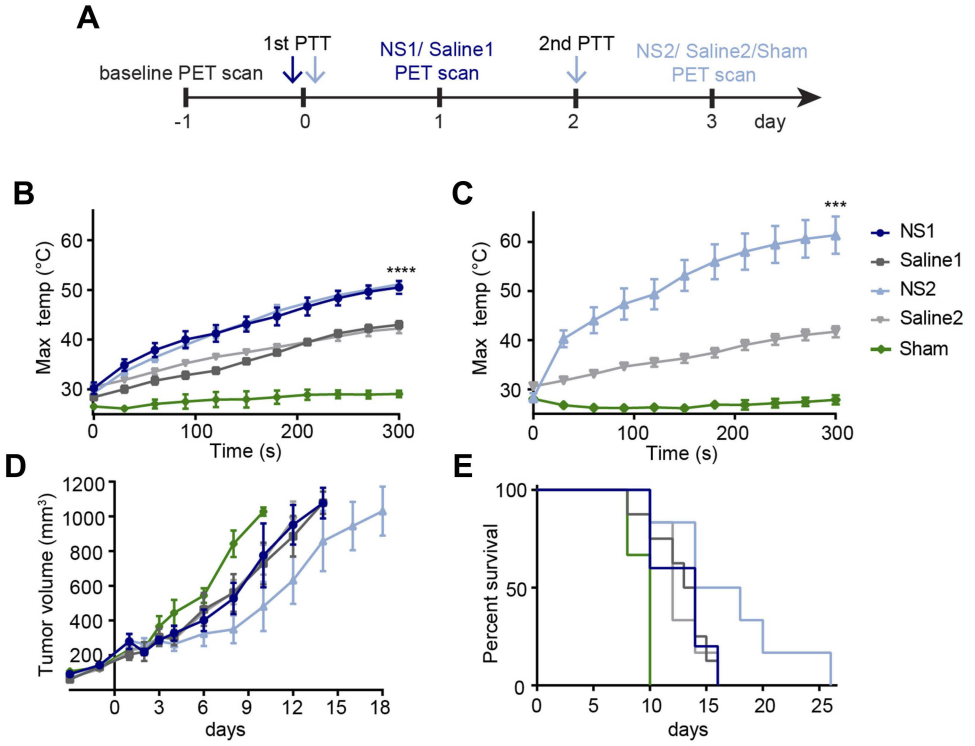

Figure 3 Temperature response and treatment outcome using two doses of laser irradiation. (**A**) Experimental timeline, which includes a standard protocol receiving one laser treatment on day 0 (dark blue) and a two-dose protocol receiving laser treatment on day 0 and day 2 (light blue). Both protocols consist of NS-laden tumors (group receiving one dose: NS1, n=5; group receiving two doses: NS2, n=6), saline groups (group receiving one dose: Saline1, n=8; group receiving two doses: Saline2, n=6) and a sham group (group receiving NS but no laser treatment, n=6). All animals are ^{18}FDG PET/CT scanned the day before the first PTT and 1 day after their last laser treatment. (**B**) Temperature elevation during the first laser dose of all animals. The maximum temperatures reached after 5 minutes were compared. For the first treatment, both NS groups together were compared against both saline groups. **** p<0.0001, *** p<0.001. (**C**) Temperature elevation during the second laser dose. Maximum temperatures for NS2 and Saline2 were compared. (**D**) Tumor growth after treatment and (**E**) overall survival for all four groups. Tumor growth is plotted until n≥3 and data shown are mean±SEM.

Sham mice were anesthetized for 5 minutes and placed on the same treatment platform as animals in the NS and saline groups, however, with the laser turned off. For early treatment response evaluation, the mice were ^{18}F-FDG PET/CT scanned 1 day before treatment (baseline) and 1 day after their last treatment (day 1 or day 3). Sham mice were scanned on baseline and day 3.

Using real-time thermographic imaging it was observed that for the NS groups one laser treatment resulted in a maximum temperature of around 50°C, whereas a second laser treatment gave an approximately 10°C higher temperature (Figures 3B and C). For the saline groups, no differences in the maximum temperatures reached during the first and second ablation were observed. The 10°C higher temperature measured during the second treatment compared to the first treatment in the NS groups was likely due to heating of scabs on the tumors that often develop after PTT. Scabs can heat more than regular tissue, and the FLIR camera cannot distinguish the contribution of these two.

Following treatment, tumor size monitoring showed that there were no significant differences in tumor growth between the different groups, but all NS and saline groups showed inhibited tumor growth when compared to the sham group (Figure 3D). This indicated that the laser per se also had some effect. Additionally, the NS2 group did show a better survival rate compared to the other groups (hazard ratio to NS1 group=0.47, 95% CI=0.1276–1.759, p=0.1; hazard ratio to Saline1 group=0.52, 95% CI=0.1841–1.49, p=0.1; hazard ratio to Saline2 group=0.43, 95% CI=0.1251–1.476, p=0.06, and hazard ratio to sham group=0.33, 95% CI=0.09024–1.231, p=0.0054, Figure 3E). This tendency was also supported by ^{18}F-FDG PET/CT response evaluation. Figure 4A shows representative images from the ^{18}F-FDG PET/CT analysis, where the effect of the treatment in the NS2 group is clearly visualized as reduced ^{18}F-FDG uptake in the tumor. Tumor ^{18}F-FDG uptake was analyzed quantitatively and extracted as %ID/g (percentage of injected dose per gram of tissue, Figure 4B). At baseline, all groups had comparative ^{18}F-FDG uptake, which also remained at the same level in both saline groups and the sham group after treatment. After treatment, there was a small reduction of around 20% in the ^{18}F-FDG uptake for the NS1 group compared to baseline. Meanwhile, the uptake in the NS2 group was reduced significantly (around 50%) in comparison to all the other groups and to baseline levels.

The results for the NS2 group (improved survival rate and 50% decrease of ^{18}F-FDG uptake after treatment) indicated that there was some effect of giving the second treatment. In addition, we found a moderate and significant correlation between the ^{18}F-FDG uptake ratio and survival in the groups undergoing two treatments (Figure 4C; r^2=0.52, p=0.0083).

Evaluation of four-dose fractionated treatment in tumor-bearing mice

Motivated by the observation that adding a second laser treatment slowed down the tumor growth in some animals, a second study was initiated where the mice underwent four laser treatments separated by 1 day of recovery (ie, a full protocol lasted 7 days; n=6 and mean tumor size at

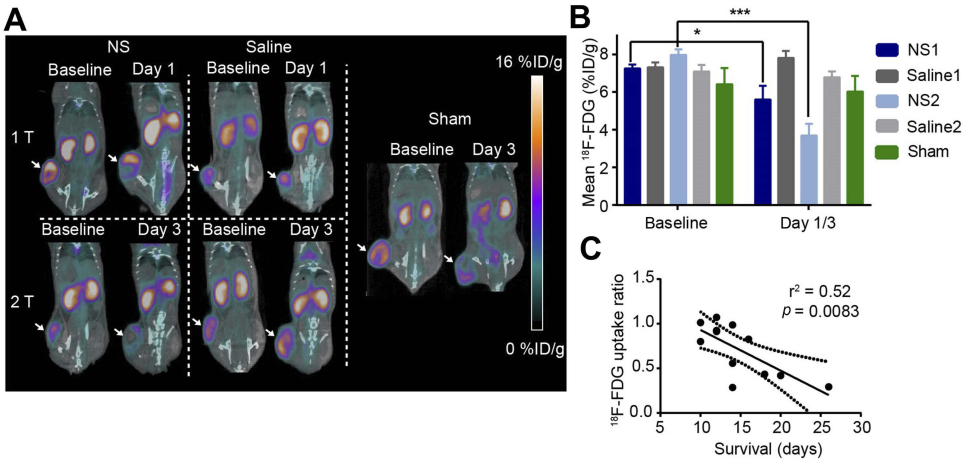

Figure 4 PET-based treatment evaluation. (**A**) Representative ^{18}F-FDG PET/CT images of NS, saline, and sham animals at baseline and after treatment. Arrows point to the tumors. 1T=1 treatment, 2T=2 treatments. (**B**) The mean tumor ^{18}F-FDG uptake at baseline and at day 1 or day 3 (NS group receiving one dose of irradiation: NS1, n=5; NS group receiving two doses of irradiation: NS2, n=6; saline group receiving one dose of irradiation: Saline1, n=8; saline group receiving two doses of irradiation: Saline2, n=6; sham group receiving NS but no irradiation: Sham, n=6). * p<0.05, *** p<0.001. Data shown are mean±SEM. (**C**) Correlation between ^{18}F-FDG uptake ratio (baseline/day 3) for animals in the NS2 and Saline2 groups.

baseline=110.3 mm^3, see Figure 5A). A control group receiving saline instead of NS was also included (n=7 and mean tumor size at baseline=132.2 mm^3). As before, all animals were ^{18}F-FDG PET/CT scanned 1 day before the first treatment (baseline) and 1 day after the last treatment (day 7).

Using thermographic imaging (Figure 5B), the maximum temperature was measured to be ~51°C (first treatment), ~49°C (second treatment), ~53°C (third treatment), and ~51°C (fourth treatment) in the NS group. These temperatures were significantly higher than the ones reached in the saline group, being ~43°C (first treatment), ~41°C (second treatment), ~42°C (third treatment), and ~40°C (fourth treatment).

Despite a good temperature increase in all four treatments, the tumor growth in the NS group did not significantly differ from the saline group (Figure 5C). In addition, the survival was also not significantly different between the two groups, although there was a tendency to increased survival in the NS group (hazard ratio of 0.56, 95% CI=0.1835–1.697, p=0.2. Figure 5D), and one NS-treated animal even showed complete removal of the tumor (this mouse was euthanized tumor-free on day 60).

^{18}F-FDG PET/CT imaging was performed on day −1 (baseline) and on day 7; representative images of the ^{18}F-FDG uptake before and after therapy are shown in Figure 6A. The quantified mean ^{18}F-FDG uptake was comparable for the two groups on baseline (Figure 6B). However, there was no significant difference at day 7, either between the two groups or compared to baseline. In spite of this, the ^{18}F-FDG uptake ratio again showed a moderate and significant correlation with survival (r^2=0.49, p=0.0109, Figure 6C).

As the treatment response was fairly close to the response from the two-dose fractionated PTT protocol, we would have expected the mean ^{18}F-FDG uptake to be similar as well. However, in both our protocols it appears that the treatment outcome is highly heterogeneous and probably dependent on how well the tumors are treated during the first and maybe second round of PTT. We suspect that the tumors that are insufficiently damaged in the beginning will also not benefit from subsequent treatments and recover within a week or so. Hence, the lack of change in mean ^{18}F-FDG uptake probably reflects that only two out of six animals showed increased survival (see Figure 5D), and that the early effect of PTT on ^{18}F-FDG uptake cannot be seen at a day 7 scan.

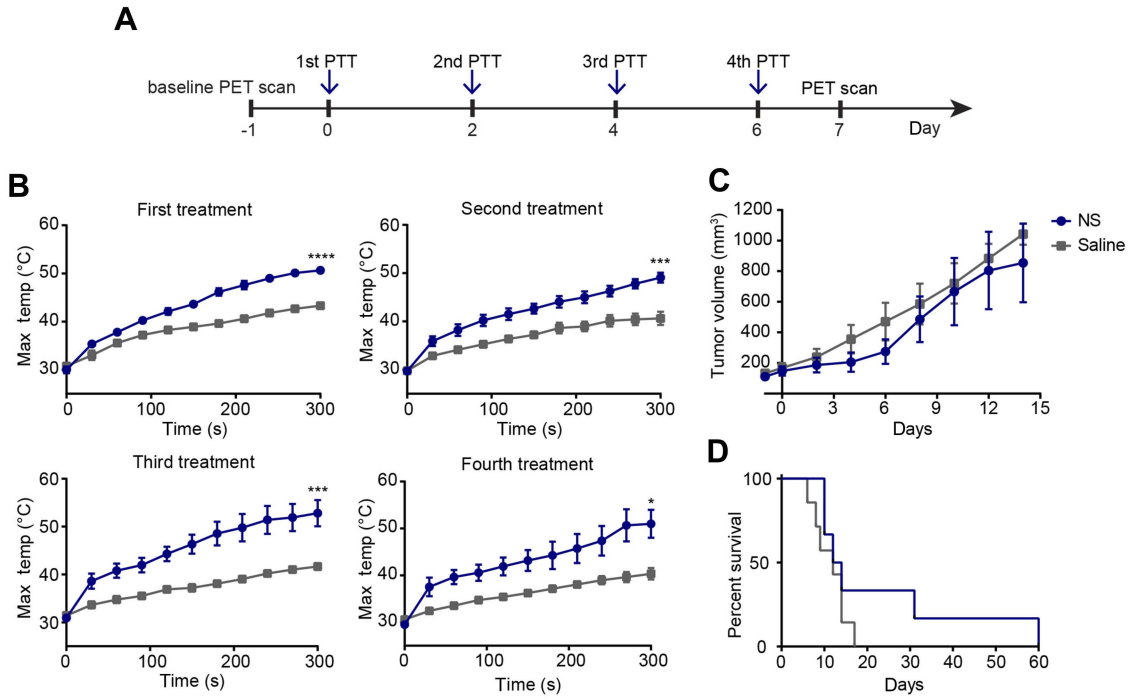

Figure 5 Temperature response and treatment outcome using four doses of laser irradiation. (**A**) Experimental timeline where the protocol consists of two groups receiving either NS or saline which were laser treated four times with 1 day in between treatments. All animals were baseline scanned the day before PTT and 1 day after their last PTT. (**B**) Temperature elevation during all four laser treatments in NS-laden tumors (NS, n=6) and the control group (Saline, n=7). The maximum temperatures reached at the last time point (300 s) were compared. * p<0.05, ** p<0.01, and *** p<0.001. (**C**) Tumor growth after treatment, and (**D**) overall survival for both groups. Day 60 was considered the end of the study. Tumor growth is plotted until n≥3 and data shown are mean±SEM.

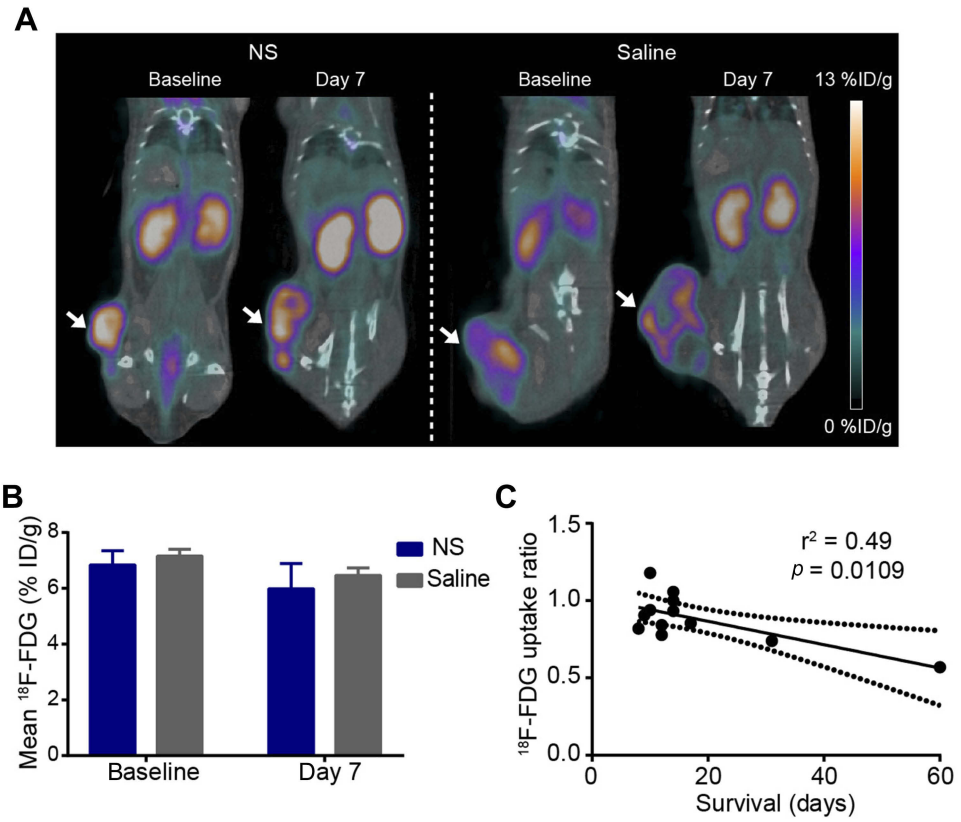

Figure 6 PET-based treatment evaluation. (**A**) Representative ^{18}F-FDG PET/CT images of NS and saline-treated animals at baseline and after treatment. Arrows point to the tumors. (**B**) The mean ^{18}F-FDG tumor uptake at baseline and day 7 (NS group, n=6; saline group, n=6). Data shown are mean±SEM. (**C**) Correlation between ^{18}F-FDG uptake ratio (baseline/day 7) and survival for animals in the NS and saline groups.

Discussion

PTT relies on the ability of heat-generating nanoparticles to selectively destroy malignant tissue when irradiated with light, sparing surrounding healthy tissue. So naturally optimizing the nanoparticle design, such that they accumulate efficiently in tumors and generate light-induced hyperthermic temperatures, has been the main focus in the field. At this point, however, it is becoming more and more evident that optimizing the nanoparticles can only improve the treatment outcome so much, and efficacy studies in particular in larger tumors are not looking very promising with regard to PTT as a standalone therapy.[15,27,33] In contrast, the application of PTT in combination with other therapies offers many opportunities to obtain synergistic effects, and, hence, suggests that the treatment protocol rather than the nanoparticles needs optimization at this stage. A few studies using fractionated PTT in mice have shown promising results,[22–24] and motivated by this we decided to evaluate two protocols where tumor-bearing animals received either two or four laser treatments, respectively.

First, we validated in vitro that the NS in aqueous solutions could be heated at low laser irradiation, also repeatedly. It is commonly seen in PTT that the laser in itself induces a temperature increase of up to ~10°C.[27,38] To attempt to reduce this, we applied glycerol to the tumor surface, an index matching agent, and found that it could reduce the laser-induced heating rate as well as suppress unspecific heating. The effect was found to be more prominent in larger tumors. Consequently, glycerol was employed in all animal studies.

Despite reaching temperatures sufficient for tissue ablation in both fractionated PTT studies, the response was only modest, and the number of laser treatments did not have a significant impact on tumor growth. Based on these observations, we first of all speculate that thermographic imaging might not be a suitable method for tumor-temperature detection in fractionated PTT protocols, since the measurements more likely represent the heating of developed scabs, than elevated intratumoral temperatures.

The response was, however, fairly heterogeneous, and a few animals did live longer in the groups receiving two

or four laser treatments, resulting in improved survival rates compared to the group that only received a single treatment. One mouse in the four-treatment group even experienced complete tumor regression. The group sizes in this study were comparable to other studies on PTT and fractionated therapy.[23,24] However, it should be noted that at these group sizes the risk of type II statistical errors make detection of smaller survival benefits difficult to show.

Our findings are in contrast to another study conducting fractionated PTT in mice which reported great response after four treatments using a laser intensity even lower than the one used in this study, although in smaller tumors.[23] Hence, there are probably many factors that can contribute to the treatment outcome, such as choice of photothermal agent, tumor size at initiation of treatment, laser dose, and treatment protocol. Also, the tumor model we used in our study is rather fast-growing and it is likely that fractionated PTT could be more efficient in a less aggressive and slower-growing tumor.

Another study in the literature conducting fractionated PTT reported loss of effect after the first treatment, probably owing to the clearance of nanoparticles from the tumor.[24] They were, however, able to solve this issue using a spatially stable hydrogel that, after four treatments, showed effective tumor suppression. It is possible that our protocols, especially the one with four-treatments, also suffer from tumor clearance of NS, and perhaps the outcome could be improved if the animals were administered with a second dose of nanoparticles during the treatment period. However, treatment-induced edema or vessel destruction in the tumor can be expected after therapy,[39] and this will impair the tumor uptake of nanoparticles. Also, nanoparticles are commonly coated with polyethylene glycol (PEG) to improve blood circulation, but this has been reported to induce an immune response and accelerated clearance if administered multiple times.[40–42] Therefore, it could also be of interest to evaluate nanoshells functionalized with other types of coating than PEG.[43,44]

Overall, fractionated PTT has only been applied in a few studies, and more knowledge about how to optimize the treatment protocol, eg number of treatments, laser dose, duration, and appropriate tumor models, is needed. Additionally, the use of thermographic imaging to measure tumor temperatures might not be appropriate for detecting the effect of PTT when working with multiple treatments. Thus, other non-invasive imaging techniques such as PET/CT imaging could be more suitable for evaluating and optimizing treatment protocols for fractionated PTT.

Conclusion

Overall, in this study we found no significant difference in outcome between groups receiving PTT to tumors in fractions compared to a single-dose approach, despite achieving temperatures during laser irradiation that were above the limit for induction of irreversible damage. Nevertheless, the outcome was heterogeneous, and a few animals did respond to fractionated therapy, resulting in improved survival rates compared to single-dose or control-treated animals. In addition, we also found that therapy-induced changes in ^{18}F-FDG uptake correlated with survival, and we suggest that ^{18}F-FDG PET/CT imaging may be used for guiding the number of treatment sessions necessary.

Acknowledgments

This project received funding from the European Research Council (ERC) under the European Union's Horizon 2020 research and innovation programme (grant agreement No 670261), the H2020 programme, the Lundbeck Foundation, the Novo Nordisk Foundation, the Innovation Fund Denmark, the Danish Cancer Society, Arvid Nilsson Foundation, Svend Andersen Foundation, the Neye Foundation, the Research Foundation of Rigshospitalet, the Danish National Research Foundation (grant 126), the Research Council of the Capital Region of Denmark, and the Research Council for Independent Research.

We acknowledge the assistance from the Core Facility for Integrated Microscopy, Faculty of Health and Medical Sciences, University of Copenhagen.

Disclosure

Ms Marina Simón, Dr Kamilla Norregaard, and Dr Jesper Tranekjær Jørgensen report grants from Novo Nordisk Foundation, European Research Council, Lundbeck Foundation, Innovation Fund Denmark, Danish Cancer Society, Arvid Nilsson Foundation, Svend Andersen Foundation, Neye Foundation, Research Foundation from Rigshospitalet, Research Council for Independent Research, Research Council of the Capital Region of Denmark, and Danish National Research Foundation, during the conduct of the study. Professor Lene Broeng Oddershede and Professor Andreas Kjaer report no conflicts of interest in this work.

References

1. Shi J, Kantoff PW, Wooster R, Farokhzad OC. Cancer nanomedicine: progress, challenges and opportunities. *Nat Rev Cancer*. 2017;17(1):20–37. doi:10.1038/nrc.2016.108
2. Hare JI, Lammers T, Ashford MB, Puri S, Storm G, Barry ST. Challenges and strategies in anti-cancer nanomedicine development: an industry perspective. *Adv Drug Deliv Rev*. 2017;108:25–38. doi:10.1016/J.ADDR.2016.04.025
3. de Melo-Diogo D, Pais-Silva C, Dias DR, Moreira AF, Correia IJ. Strategies to improve cancer photothermal therapy mediated by nanomaterials. *Adv Healthc Mater*. 2017;6:10. doi:10.1002/adhm.201700073
4. Jaque D, Martínez Maestro L, Del Rosal B, et al. Nanoparticles for photothermal therapies. *Nanoscale*. 2014;6(16):9494–9530. doi:10.1039/c4nr00708e
5. Jacques SL. Optical properties of biological tissues: a review. *Phys Med Biol*. 2013;58(11):R37–R61. doi:10.1088/0031-9155/58/11/R37
6. Matsumura Y, Maeda H. A new concept for macromolecular therapeutics in cancer chemotherapy: mechanism of tumoritropic accumulation of proteins and the antitumor agent smancs. *Cancer Res*. 1986;46(12Part 1). Available from: http://cancerres.aacrjournals.org/content/46/12_Part_1/6387. Accessed July 15, 2017.
7. Greish K. Enhanced Permeability and Retention (EPR) effect for anticancer nanomedicine drug targeting. In: Grobmyer SR, Moudgil BM, editors. *Cancer Nanotechnology: Methods and Protocols*. Totowa (NJ): Humana Press; 2010:25–37. doi:10.1007/978-1-60761-609-2_3
8. Jhaveri AM, Torchilin VP. Multifunctional polymeric micelles for delivery of drugs and siRNA. *Front Pharmacol*. 2014;5 APR. doi:10.3389/fphar.2014.00077
9. Chen Q, Xu L, Liang C, Wang C, Peng R, Liu Z. Photothermal therapy with immune-adjuvant nanoparticles together with checkpoint blockade for effective cancer immunotherapy. *Nat Commun*. 2016;7:13193. doi:10.1038/ncomms13193
10. Gobin AM, Watkins EM, Quevedo E, Colvin VL, West JL. Near-infrared-resonant gold/gold sulfide nanoparticles as a photothermal cancer therapeutic agent. *Small*. 2010;6(6):745–752. doi:10.1002/smll.200901557
11. Stern JM, Stanfield J, Kabbani W, Hsieh J-T, Cadeddu JA. Selective prostate cancer thermal ablation with laser activated gold nanoshells. *J Urol*. 2008;179(2):748–753. doi:10.1016/j.juro.2007.09.018
12. Day ES, Thompson PA, Zhang L, et al. Nanoshell-mediated photothermal therapy improves survival in a murine glioma model. *J Neurooncol*. 2011;104(1):55–63. doi:10.1007/s11060-010-0470-8
13. O'Neal DP, Hirsch LR, Halas NJ, Payne JD, West JL. Photo-thermal tumor ablation in mice using near infrared-absorbing nanoparticles. *Cancer Lett*. 2004;209(2):171–176. doi:10.1016/J.CANLET.2004.02.004
14. Chatterjee DK, Diagaradjane P, Krishnan S. Nanoparticle-mediated hyperthermia in cancer therapy. *Ther Deliv*. 2011;2(8):1001–1014. doi:10.4155/tde.11.72
15. Ayala-Orozco C, Urban C, Bishnoi S, et al. Sub-100 nm gold nanomatryoshkas improve photo-thermal therapy efficacy in large and highly aggressive triple negative breast tumors. *J Control Release*. 2014;191:90–97. doi:10.1016/j.jconrel.2014.07.038
16. Hirsch LR, Stafford RJ, Bankson JA, et al. Nanoshell-mediated near-infrared thermal therapy of tumors under magnetic resonance guidance. *Proc Natl Acad Sci*. 2003;100(23):13549–13554. doi:10.1073/PNAS.2232479100
17. Sato K, Sato N, Xu B, et al. Spatially selective depletion of tumor-associated regulatory T cells with near-infrared photoimmunotherapy. *Sci Transl Med*. 2016;8(352):352ra110LP–352ra110. doi:10.1126/scitranslmed.aaf0746
18. Bear AS, Kennedy LC, Young JK, et al. Elimination of metastatic melanoma using gold nanoshell-enabled photothermal therapy and adoptive T cell transfer. Najbauer J, ed. *PLoS One*. 2013;8(7):e69073. doi:10.1371/journal.pone.0069073
19. Piao J-G, Gao F, Yang L. Acid-responsive therapeutic polymer for prolonging nanoparticle circulation lifetime and destroying drug-resistant tumors. *ACS Appl Mater Interfaces*. 2016;8(1):936–944. doi:10.1021/acsami.5b10550
20. Piao J-G, Liu D, Hu K, et al. Cooperative Nanoparticle System for Photothermal Tumor Treatment without Skin Damage. *ACS Appl Mater Interfaces*. 2016;8(4):2847–2856. doi:10.1021/acsami.5b11664
21. Dombrovsky L, Timchenko V, Jackson M. *Indirect Heating Strategy of Laser Induced Hyperthermia: An Advanced Thermal Model*. Vol. 55; 2012. doi:10.1016/j.ijheatmasstransfer.2012.04.029
22. El-Sayed MA, Ali M, Ibrahim I, Ali H, Selim S. Treatment of natural mammary gland tumors in canines and felines using gold nanorods-assisted plasmonic photothermal therapy to induce tumor apoptosis. *Int J Nanomedicine*. 2016;11:4849–4863. doi:10.2147/IJN.S109470
23. Gutwein LG, Singh AK, Hahn MA, et al. Fractionated photothermal antitumor therapy with multidye nanoparticles. *Int J Nanomedicine*. 2012;7:351–357. doi:10.2147/IJN.S26468
24. Hsiao CW, Chuang EY, Chen HL, et al. Photothermal tumor ablation in mice with repeated therapy sessions using NIR-absorbing micellar hydrogels formed in situ. *Biomaterials*. 2015;56:26–35. doi:10.1016/j.biomaterials.2015.03.060
25. Dombrovsky LA, Timchenko V, Jackson M, Yeoh GH. A combined transient thermal model for laser hyperthermia of tumors with embedded gold nanoshells. *Int J Heat Mass Transf*. 2011;54(25):5459–5469. doi:10.1016/j.ijheatmasstransfer.2011.07.045
26. Ren Y, Qi H, Chen Q, Ruan L. Thermal dosage investigation for optimal temperature distribution in gold nanoparticle enhanced photothermal therapy. *Int J Heat Mass Transf*. 2017;106(C):212–221. doi:10.1016/j.ijheatmasstransfer.2016.10.067
27. Jørgensen JT, Norregaard K, Simón Martín M, Oddershede LB, Kjaer A. Non-invasive early response monitoring of nanoparticle-assisted photothermal cancer therapy. *Nanotheranostics*. 2018;2(3):201–210. doi:10.7150/ntno.24478
28. Jørgensen JT, Nørregaard K, Tian P, Bendix PM, Kjaer A, Oddershede LB. Single particle and PET-based platform for identifying optimal plasmonic nano-heaters for photothermal cancer therapy. *Sci Rep*. 2016;6:30076. doi:10.1038/srep30076
29. Pilot study of AuroLase™ therapy in refractory and/or recurrent tumors of the head and neck [Internet]. Available from: http://clinicaltrials.gov/ct2/show/NCT00848042 Accessed May 20, 2019.
30. Pedrosa P, Vinhas R, Fernandes A, Baptista P. Gold nanotheranostics: proof-of-concept or clinical tool? *Nanomaterials*. 2015;5(4):1853–1879. doi:10.3390/nano5041853
31. MRI/US fusion imaging and biopsy in combination with nanoparticle directed focal therapy for ablation of prostate tissue [Internet]. Available from: https://clinicaltrials.gov/ct2/show/NCT02680535 Accessed May 20, 2019.
32. Gad SC, Sharp KL, Montgomery C, Payne JD, Goodrich GP. Evaluation of the toxicity of intravenous delivery of auroshell particles (Gold–silica Nanoshells). *Int J Toxicol*. 2012;31(6):584–594. doi:10.1177/1091581812465969
33. Norregaard K, Jørgensen JT, Simón M, et al. 18F-FDG PET/CT-based early treatment response evaluation of nanoparticle-assisted photothermal cancer therapy. *PLoS One*. 2017;12(5):e0177997. doi:10.1371/journal.pone.0177997
34. Ayala-Orozco C, Urban C, Knight MW, et al. Au nanomatryoshkas as E ffi cient transducers for cancer treatment: benchmarking against nanoshells. *ACS Nano*. 2014;8(6):6372–6381. doi:10.1021/nn501871d
35. Jirkof P, Tourvieille A, Cinelli P, Arras M. Buprenorphine for pain relief in mice: repeated injections vs sustained-release depot formulation. *Lab Anim*. 2014;49(3):177–187. doi:10.1177/0023677214562849
36. Kang X, Guo X, An W, et al. Photothermal therapeutic application of gold nanorods-porphyrin-trastuzumab complexes in HER2-positive breast cancer. *Sci Rep*. 2017;7:1–14. doi:10.1038/srep42069

37. Liu H, Chen D, Tang F, et al. Photothermal therapy of Lewis lung carcinoma in mice using gold nanoshells on carboxylated polystyrene spheres. *Nanotechnology*. 2008;19(45):455101. doi:10.1088/0957-4484/19/45/455101
38. Lin KY, Bagley AF, Zhang AY, Karl DL, Yoon SS, Bhatia SN. Gold nanorod photothermal therapy in a genetically engineered mouse model of soft tissue sarcoma. *Nano Life*. 2010;1(03n04):277–287. doi:10.1142/S1793984410000262
39. Yang TD, Choi W, Yoon TH, et al. In vivo photothermal treatment by the peritumoral injection of macrophages loaded with gold nanoshells. *Biomed Opt Express*. 2016;7(1):185–193. doi:10.1364/BOE.7.000185
40. Yang Q, Lai SK. Anti-PEG immunity: emergence, characteristics, and unaddressed questions. *Wiley Interdiscip Rev Nanomed Nanobiotechnol*. 2015;7(5):655–677. doi:10.1002/wnan.1339
41. Abu Lila AS, Kiwada H, Ishida T. The accelerated blood clearance (ABC) phenomenon: clinical challenge and approaches to manage. *J Control Release*. 2013;172(1):38–47. doi:10.1016/j.jconrel.2013.07.026
42. Laverman P, Carstens MG, Boerman OC, et al. Factors affecting the accelerated blood clearance of polyethylene glycol-liposomes upon repeated injection. *J Pharmacol Exp Ther*. 2001;298(2):607–612. Available from: http://www.ncbi.nlm.nih.gov/pubmed/11454922.
43. Piao J-G, Wang L, Gao F, You Y-Z, Xiong Y, Yang L. Erythrocyte membrane is an alternative coating to polyethylene glycol for prolonging the circulation lifetime of gold nanocages for photothermal therapy. *ACS Nano*. 2014;8(10):10414–10425. doi:10.1021/nn503779d
44. Strong LE, West JL. Hydrogel-coated near infrared absorbing nanoshells as light-responsive drug delivery vehicles. *ACS Biomater Sci Eng*. 2015;1(8):685–692. doi:10.1021/acsbiomaterials.5b00111